The crystal–liquid interface of a body-centered-cubic-forming substance: Computer simulations of the r^{-6} potential

Brian B. Laird[a] and A. D. J. Haymet[b]
Department of Chemistry, University of California, Berkeley, California 94720

(Received 13 March 1989; accepted 6 June 1989)

The interfaces between a bcc crystal and its melt are studied by molecular dynamics simulation. Three distinct crystal/melt interfaces, (100), (111), and (110) are studied. For all interfaces the variation with z, the coordinate perpendicular to the interfacial plane, of the single particle density (averaged over the directions perpendicular to z) and the diffusion constant are measured. Although the 10–90 widths of the density peak-height profiles differ significantly among the three interfaces (6, 9, and 7 molecular diameters, respectively), the corresponding 10–90 widths of the diffusion constant profiles are nearly identical with a common value of about four molecular diameters. This leads to the conclusion that the differences in apparent structural width are due primarily to geometric considerations and not to differences in average local molecular environments.

I. INTRODUCTION

The structure and dynamics of an interface between a crystal and its melt are of paramount importance in studies of crystal growth near equilibrium. Such an interface lies between two condensed phases making direct experimental study difficult.[1] While laboratory estimates of the surface excess free energy for a limited number of systems have been obtained both directly and indirectly,[2–6] experimental data concerning the microscopic structure of the interfacial region is lacking. This experimental difficulty increases the role of computer simulation in the development of a suitable interface theory.

Some previous simulations treat the interface as a liquid up against a hard wall or rigid crystal face. These include hard sphere models[7] as well as molecular dynamics simulations.[8] The perturbation theory of Abraham and Singh has been used to describe this type of interface.[9] This approach causes the interfacial width to be consistently underestimated, because it does not take into account the participation of the crystal. Several recent simulations have addressed the situation in which both the liquid and solid participate in forming the interfacial region.[10–15] With the exception of the recent simulations of the ice/water interface by Karim and Haymet[15] and some simulations of the silicon interfaces,[16] all of these involve face-centered-cubic (fcc) crystal faces and most (except Ref. 11) employ the Lennard-Jones interaction potential. The density profiles and diffusion constant profiles through the interface, both important for the development of theories of crystal growth dynamics,[17] have been calculated for several fcc faces. These profiles show that the interface is diffuse, with the interfacial region extending over 7–10 crystal layers perpendicular to the interface. Estimation of the surface excess free energy has been attempted, but has met with limited success to date.[13]

In this paper, we present the first such simulations involving body-centered-cubic (bcc) crystal faces. The motivation for such a study is that bcc is one of the simplest, commonly occurring, non-close-packed crystal structures, and, as such, is a natural choice for extending the available simulation data beyond the close-packed systems.

The current simulations use the technique of constant energy and volume molecular dynamics.[18–23] Specifically, the velocity-Verlet algorithm of Swope *et al.*[24] is employed. The system under study is one made up of particles interacting via a spherically symmetric, pairwise-additive and purely repulsive interatomic potential

$$v(r) = \epsilon \left(\frac{\sigma}{r}\right)^6 . \tag{1}$$

(In order to prevent excess energy drift, a function of the form $A + Br^2$ was added to the potential [Eq. (1)], where A and B were chosen so that both the potential and force are zero at the neighbor table cutoff separation of 2.5σ). This particular form for the potential was chosen for two reasons. First, the inverse-power form of the potential results in scaling relations from which the thermodynamic properties of any point on the solid–liquid coexistence line can be calculated from data at a single point on that line.[25] These relations stem from the fact that the natural energy scale ϵ and the natural length scale σ are not independent because only the combination $\epsilon\sigma^6$ appears in the potential [Eq. (1)]. Secondly, the sixth power is apparently the highest integer power (shortest-range) potential that freezes into a bcc solid.[26] It should be noted that the soft-sphere potential chosen here is not intended to represent any specific class of substances in the same way that the Lennard-Jones potential is a representation of the noble gas potentials. It is primarily a convenient theoretical model. It is not unreasonable to assume, however, that the results of these simulations can be used to interpret qualitatively the interfacial properties of simple, bcc-

[a] Present address: Institut für Festkörperforschung der Kernforschungsanlage Jülich GmbH, Postfach 1913, D-5170 Jülich 1, Federal Republic of Germany.
[b] Present address and address for correspondence: Department of Chemistry, University of Utah, Salt Lake City, UT 84112.

 0021-9606/89/183638-09$02.10

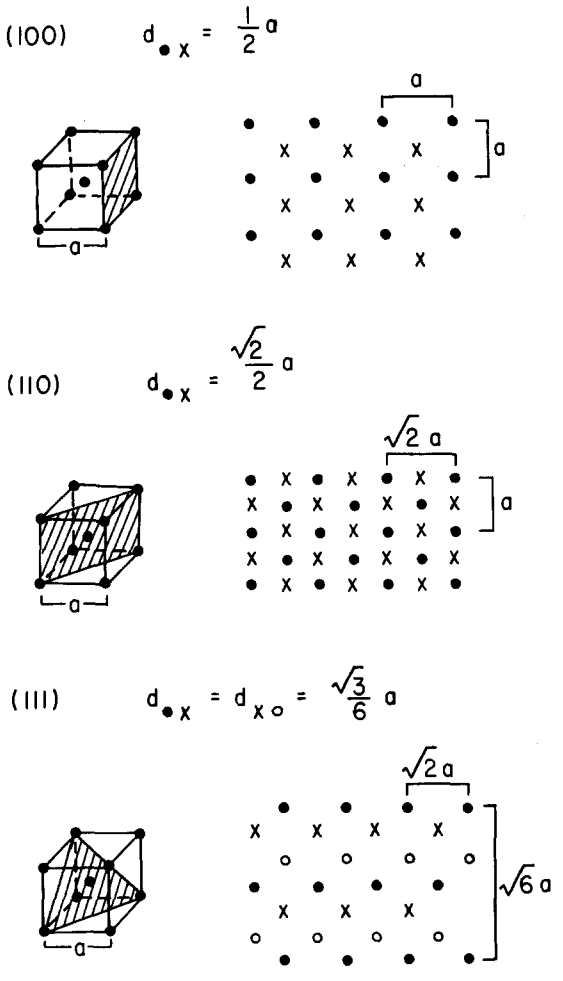

FIG. 1. Illustration of the (100), (110), and (111) interfaces in relation to the bcc unit cell. The quantity $d_{\bullet\times}$ is the distance between the ● and × crystal planes for each interface.

forming substances, such as the alkali metals.

The results of these simulations for the bcc (100), (110), and (111) interfaces are presented in Secs. II, III, and IV, respectively. (For reference, the details of the interfacial packing and the relationship to the bcc unit cell are illustrated for these three interfacial directions in Fig. 1). The principal quantities calculated are (a) the density and (b) the diffusion constant profiles as a function of perpendicular distance through each interface, yielding two different measures (one structural and one transport) of the interfacial width. For the (100) interface, two simulations differing in total number of particles are reported to estimate system size effects. The details of each simulation are also summarized in Table I. In Sec. V, these simulation results are discussed with reference to theoretical predictions from density functional theory (DFT)[27] and recent refinements to it.[28–30] In Sec. VI, our conclusions are collected.

II. SIMULATION RESULTS FOR THE (100) INTERFACE

A. Smaller (100) simulation—2160 particles

Two separate simulations of the (100) interface (one of 2160 particles and a larger one of 3430 particles) have been performed, in order to serve as a partial test of system size effects. The smaller (100) interfacial system was built from five blocks of 432 particles each for a total of 2160 particles. The details of this simulation were summarized earlier in a conference proceeding[31] but will be expanded here for the sake of completeness. Three of the blocks were set up in a bcc solid configuration with the z axis perpendicular to a (100) crystal face. The solid had a density $\rho\sigma^3 = 0.7$ with an average temperature of $kT/\epsilon = 0.1$. The two remaining blocks consisted of liquid equilibrated at the same average tempera-

TABLE I. Summary of the liquid/crystal bcc interface simulations.

Parameter	$(100)_{small}$	$(100)_{large}$	(110)	(111)
Total number of particles	2160	3430	3500	3600
No. of initial crystal particles	1296	2058	2100	2160
No. of initial liquid particles	864	1378	1400	1440
x direction box length (σ)	8.5139	9.9329	9.9329	10.0337
y direction box length (σ)	8.5139	9.9329	10.0337	10.4274
z direction box length (σ)	42.8834	50.0214	50.5418	49.5175
Volume of box (σ^3)	3108.47	4935.22	5037.18	5180.79
xy cross sectional area (σ^2)	72.486	98.622	99.664	104.625
No. of particles/crystal plane	36	49	70	30
Density of each crystal plane (particles/σ^2)	0.4966	0.4966	0.7024	0.2867
Distance between crystal planes (σ)	0.7095	0.7095	1.0034	0.4096
No. of bins for density profile	1300	2000	2000	2000
No. of bins for diffusion profile	30	60	60	60
No. of particles/diffusion bin	70	57	58	60
Length of run for averages (time units)	100	80	40	160
Average temperature (in units of ϵ/k)[a]	0.100(2)	0.097(3)	0.097(3)	0.097(2)
10–90 width-density (σ)[a]	5.7(5)	6.4(5)	9.0(5)	7.0(5)
10–90 width-diffusion (σ)[a]	3.9	3.8	3.9	4.0

[a] The quantity in brackets is the estimated error in the last digit shown.

ture but with a density $\rho_L \sigma^3 = 0.687$. The values of the temperature and densities were chosen so that system lies on the phase coexistence line as estimated by Monte Carlo simulation of the bulk properties of inverse-power potentials.[26] The blocks were placed end to end in the z direction with the three solid blocks in the middle and a liquid block on each end. Periodic boundary conditions were then applied in all three Cartesian directions. If the simulation were turned on fully at this point, the interface would not be stable because the liquid has not been equilibrated next to a solid block. This results in high energy interactions at the interface. In order to create a stable interface, the following procedure was adopted. First, the solid particles were held fixed while the liquid particles were allowed to evolve for 5400 time steps of length δt, where

$$\delta t = 0.01(m\sigma^2/\epsilon)^{1/2}. \tag{2}$$

(For example, if one uses the reasonable values for a liquid metal of 100 K, 3.5 Å and 30 amu for ϵ/k, σ and m, respectively, the reduced time step used above corresponds to approximately 20 fs). During this part of the preparation, the liquid temperature was rescaled periodically to the coexistence temperature. The solid atoms were then given their original velocities and allowed to move. The system was then equilibrated for 1000 time steps. The system at this point had a relatively flat temperature profile through the interface, which is one condition for phase coexistence. The average reduced temperature (kT/ϵ) for this (100) interfacial system was 0.100 with fluctuations on the order of 0.002.

Once a stable interface was created by the above procedure, the simulation was run for 10 000 more time steps (200 ps using the above typical parameters) to collect averages. This 10 000 step run was built from five successive runs of 2000 steps each. Analysis of the smaller runs showed that the interface was stationary for the entire period over which the averages were taken, thus ruling out the possibility of artificial interfacial broadening due to translational motion of the interfacial region. Similar analyses of the simulation runs for the other interfaces studied in this work yielded the same conclusion. The density profile for the (100) interface was calculated by dividing the z direction into 1300 bins, counting the number of particles in each bin, and dividing by the volume of the bin. Since the simulation involved two interfaces, one on each side of the solid, a center of symmetry was found so that the profile could be folded over to give an average of the two interfaces. The results of this procedure can be seen in Fig. 2. One measure of the width of the interface is the 10–90 width of the height of the density peaks. The 10–90 width of any interfacial order parameter is the distance over which the value of the quantity changes from 10% to 90% of its value in the bulk solid as one traverses the interface from the liquid into the solid. A more standard measure is the 10–90 width of the bulk density change, but, because the fractional density change for this system is only 1.3%, this profile cannot be resolved in the present simulations, given the fluctuations in the measured density profile. The 10–90 width of the peak heights will probably be greater than that for the bulk density change alone, because there is some preliminary theoretical evidence that the profiles of the nonzero wave vector Fourier components of the density are somewhat broader than (and shifted relative to) that of the zero wave vector component (the bulk density change).[27] For the (100) interface this 10–90 width is measured to be about 5.7σ (just over 8 lattice planes).

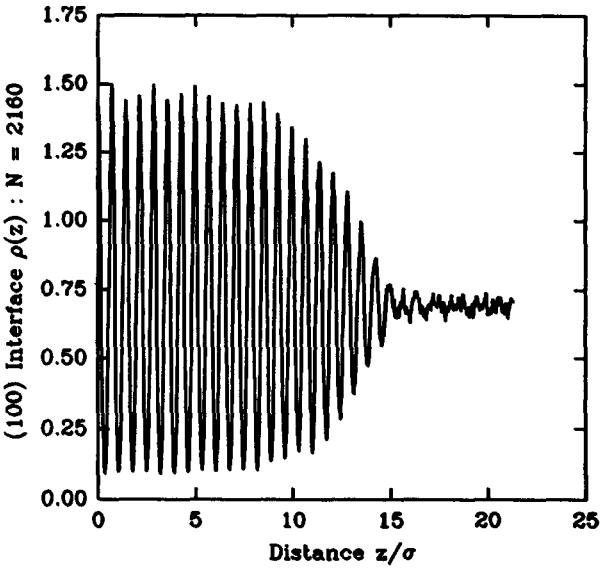

FIG. 2. The equilibrium reduced density profile $\sigma^3\rho(z)$, averaged over the perpendicular directions, of the melt/bcc (100) crystal face ($N = 2160$), as a function of distance z/σ.

The variation of the diffusion constant through the interface was calculated by dividing the z direction into 30 bins (about 70 particles per bin) and calculating the average isotropic mean squared displacement as a function of time for the particles assigned to each bin. The diffusion constant for a given bin is then calculated from the Einstein relation

$$D = \lim_{t\to\infty} \frac{\langle [\mathbf{r}(t) - \mathbf{r}(0)]^2 \rangle}{6kT}. \tag{3}$$

The measured diffusion profile as a function of distance from the solid center is shown in Fig. 3. As a test, the x–y and z components of the mean squared displacement were calculated separately for this interface, and were found not to differ measurably. The limiting liquid value of D ($0.011\,59 \pm 0.000\,01$) was obtained in a separate 686 particle simulation of the bulk liquid. Note that bulk liquid diffusion constants are known to be somewhat system size dependent.[32] Figure 4 shows the mean squared displacement curves used to calculate the diffusion profile. These curves were calculated using 50 time origins separated by 20 time steps. Least squares linear regression was used to determine the slope. In each case, the 2σ error in the slope was less than 10^{-4}. An eyeball estimate of the 10–90 width of this diffusion profile gives about 3.9σ or 5.5 lattice planes. Even considering the large error in this estimation, the diffusion width is significantly smaller than that of the density profile.

B. Larger (100) simulation–3430 particles

This (100) interface was built of five blocks (three solid and two liquid) of 686 particles each for a total of 3430 parti-

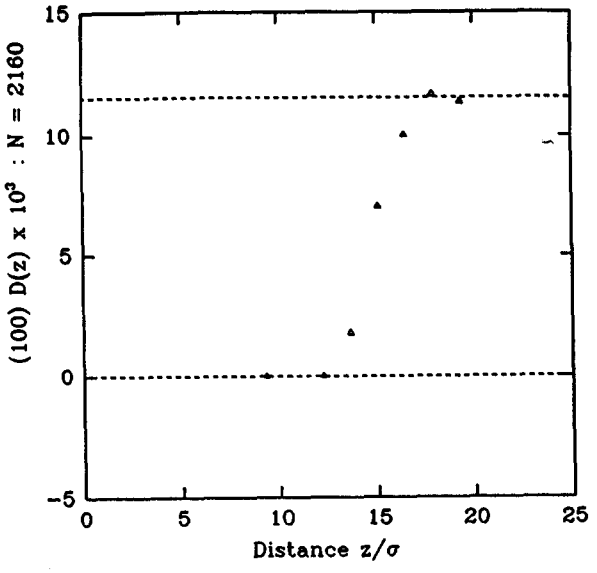

FIG. 3. The measured diffusion constant $[(\epsilon\sigma^2/m)^{1/2}\times 10^3]$ in subregions of the (100) interface ($N = 2160$). The upper dotted line is the equilibrium bulk liquid value.

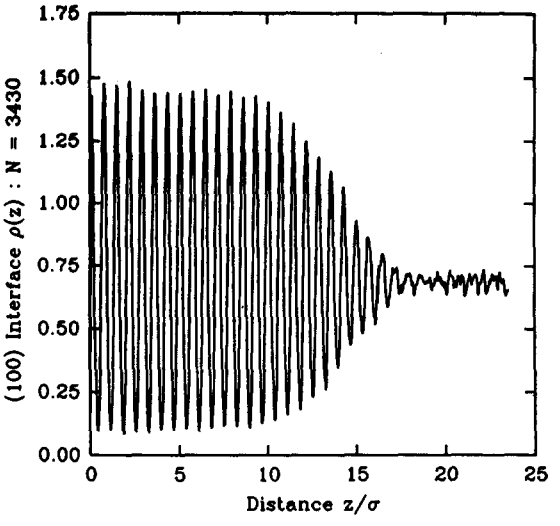

FIG. 5. The equilibrium reduced density profile $\sigma^3\rho(z)$, averaged over the perpendicular directions, of the melt/bcc (100) crystal face ($N = 3430$), as a function of distance z/σ.

cles. The magnitude of the size difference between this simulation and the smaller one described in Sec. II A above is characterized by the difference in the x–y cross section, the z-direction length and the total volume (see Table I for these values). The densities of the two simulations are identical as are the temperatures (within simulation error). The method of equilibration was the same in both simulations.

Following equilibration, this larger (100) system was evolved for 8000 time steps to collect averages. The density profile was obtained as described in Sec. II A, except that 1200 bins were used for the z-direction partition, and the resultant $\rho(z)$ is shown in Fig. 5. The 10–90 width of the peak heights is just over nine lattice planes, which corresponds to about 6.4σ units. A comparison of the density profiles for the smaller and larger (100) simulations (Figs. 2 and 5, respectively) shows that the two interfaces are essentially identical. On a finer level, the profile of the smaller system is more rounded and slightly less broad than that of the larger system. This width difference is seen in the difference between the 10–90 peak-height widths of the two systems (nine vs eight lattice planes). However, given the uncertainty of the observered interface width due to the statistical fluctuations of the peak heights, the significance of this difference is not clear. Given the general lack of knowledge as to the magnitude of the system-size effects on interfacial simulations, a clearer picture of the influence of these effects on our results for the current system would require more extensive study.

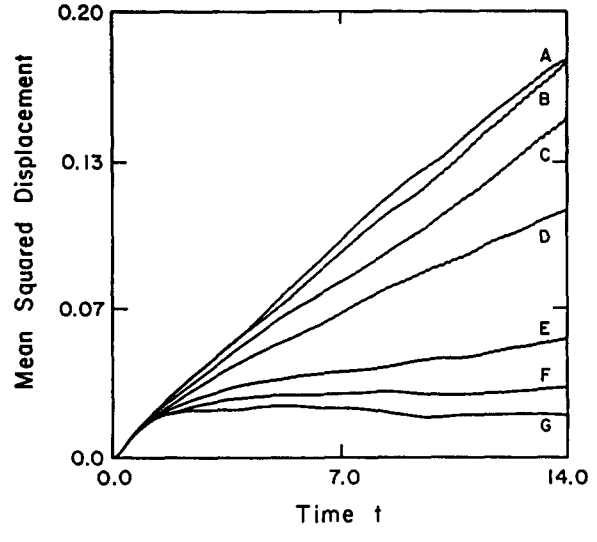

FIG. 4. The mean squared displacement (divided by 6) as a function of time of particles in subregions of the (100) interface ($N = 2160$) shown in Figs. 2 and 3.

The diffusion profile (Fig. 6) was calculated similarly to the smaller (100) interface, except that the z direction was divided into 60 bins (corresponding to 57 particles per bin on the average) instead of 30. An eyeball estimate of the 10–90 width of the diffusion profile yields about 3.8σ or about 5.4 lattice plane spacings. Although the limiting bulk liquid diffusion constant values differ by about 10%, the values for the interface widths are almost identical.

III. SIMULATION RESULTS FOR THE (110) INTERFACE

This interface was constructed from five blocks (three solid and two liquid) of 700 particles each for a total of 3500 particles. The solid blocks were oriented such that the z axis corresponds to the (110) direction of the bcc crystal. The average temperature (kT/ϵ) of the system was 0.097, with fluctuations of the order of .002. The xy cross section, unlike

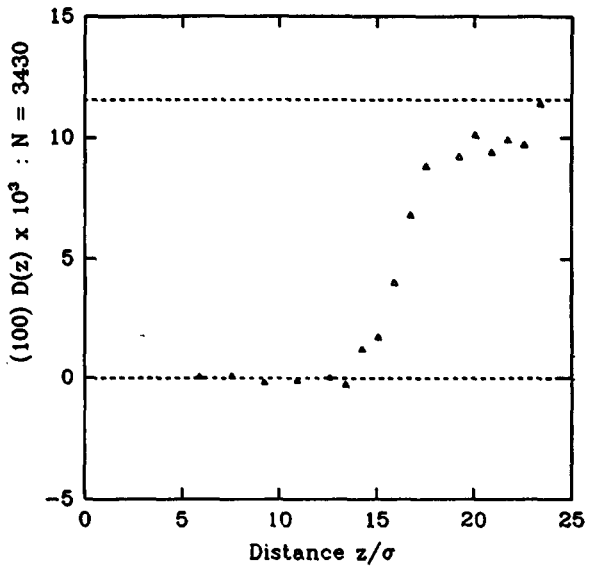

FIG. 6. The measured diffusion constant $[(\epsilon\sigma^2/m)^{1/2}\times 10^3]$ in subregions of the (100) interface ($N = 3430$). The upper dotted line is the equilibrium bulk liquid value.

that of the (100) interface, is slightly rectangular, with side lengths $xbox = 9.983$ and $ybox = 10.034$. The equilibration was performed in the same manner as for the (100) face. Once the equilibrium procedure was completed and the interface was stable, the simulation was run for 4000 time steps to collect averages. This interface requires less runtime for the averaging procedure than the (100) face because the plane particle density (see Table I and Fig. 1) is much greater (more particles per unit cross sectional area), which leads to better collection statistics. The density profile (Fig. 7) was calculated by dividing the z direction into 2000 bins. The peak height 10–90 width for this interface is about 9.0σ (nine lattice planes) indicating a broader interfacial region than in the 100 simulation.

The diffusion profile (Fig. 8) was calculated in the same manner as for the (100) interface above. In the z direction the simulation cube was divided into 60 bins (57 particles per bin) as in the large (100) simulation. A rough estimate of the diffusion 10–90 width gives about 3.9σ or 3.8 bcc (110) lattice planes. This is almost exactly the same value as for the (100) interface, which is interesting in view of the fact that the density peak 10–90 widths for the two interfaces are very different.

IV. SIMULATION RESULTS FOR THE (111) INTERFACE

The (111) interface was constructed from five blocks (three solid and two liquid) of 720 particles each for a total of 3600 particles. As for the (110) interface, the average temperature in reduced units was approximately 0.097, with fluctuations on the order of 0.002. Similarly, the x–y cross section is not square, with $xbox = 10.0337$ and $ybox = 10.4274$. Equilibration of the interface proceeded in the same manner as the (100) and (110) interfaces except that 10 000 steps were necessary to equilibrate the liquid about the fixed solid phase.

After equilibration, the simulation was run for 16 000 time steps to collect averages. Such a long averaging run, compared to the other faces, is required because the plane density of the (111) crystal planes is much lower than either the (100) or (110) planes (Table I). The lower the number of particles per unit area in a given plane, the more time steps are required to get reasonable statistics. Figure 9 shows the (111) density profile calculated by partitioning the z direction into 2000 bins. The peak height 10–90 width for the (111) interface is about 7.0σ (17 lattice planes).

As interesting feature of the (111) density profile is that

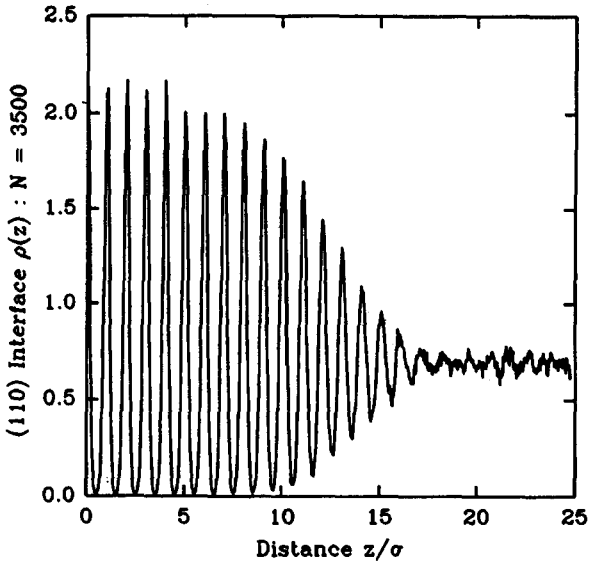

FIG. 7. The equilibrium density profile $\sigma^3\rho(z)$, averaged over the perpendicular directions, of the melt/bcc (110) crystal face, as a function of distance z/σ.

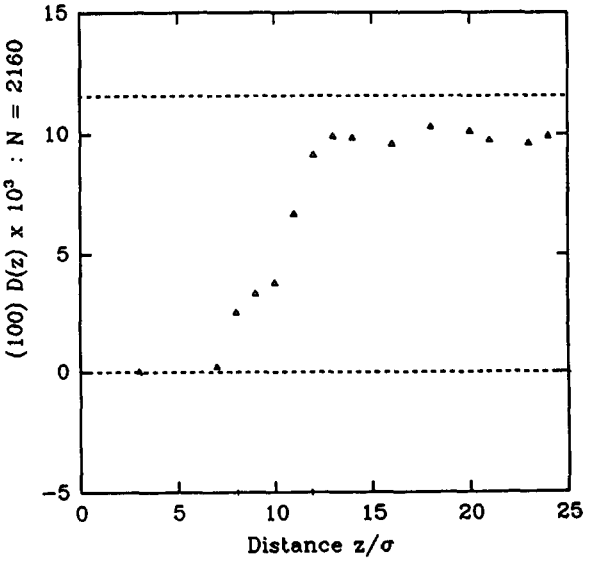

FIG. 8. The measured diffusion constant $[(\epsilon\sigma^2/m)^{1/2}\times 10^3]$ in subregions of the (110) interface. The upper dotted line is the equilibrium bulk liquid value.

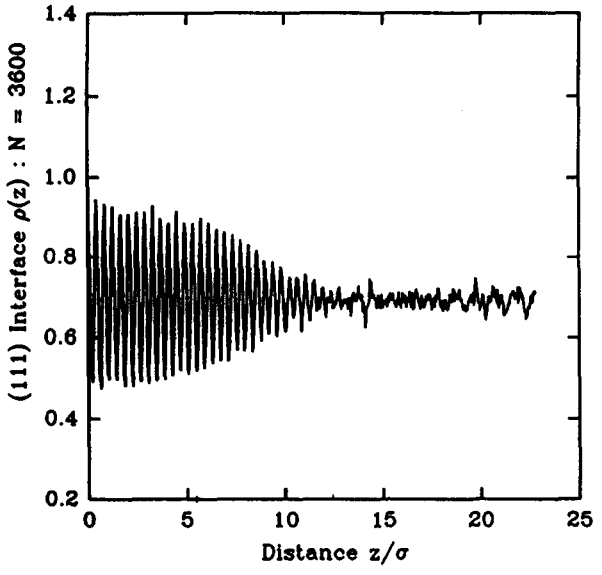

FIG. 9. The equilibrium reduced density profile $\sigma^3\rho(z)$, averaged over the perpendicular directions, of the melt/bcc (111) crystal face, as a function of distance z/σ.

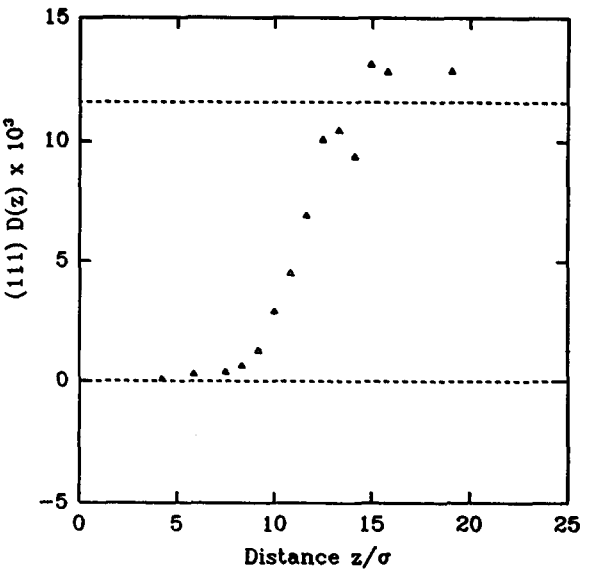

FIG. 10. The measured diffusion constant $[(\epsilon\sigma^2/m)^{1/2}\times 10^3]$ in subregions of the (111) interface. The upper dotted line is the equilibrium bulk liquid value.

the *apparent* density between the lattice planes does not drop to zero. This is also the case for the (100) interface, although to a much lesser extent. This interplane density is *not* due to the diffusion of particles from one plane into the next, but rather reflects correctly the overlap of the z axis projections of the closely spaced (111) planes. The (111) crystal direction in the bcc solid is made up of triangular lattice planes stacked upon each other, with the particles in each plane lying above the triangular holes of the previous plane in an ABCABC pattern. Since the spacing between the planes is quite small (about 0.41σ), the z coordinates of particles in two adjacent planes can overlap even though the particles remain localized about their respective lattice sites.

The diffusion profile (Fig. 10) was calculated in the same manner as for the other interfaces with the z direction being divided into 60 bins (60 particles per bin). A rough estimate of the diffusion 10–90 width gives about 4.0σ or 9.8 (111) bcc lattice planes. Again it is interesting to note that this is almost exactly the same value as for the other two interfaces. It is therefore tempting to speculate that the differences in the density profiles among these three interfaces are due primarily to geometric considerations, which do not affect the transport properties.

V. DISCUSSION AND COMPARISON WITH EXISTING THEORY

Computer simulations have a twofold role in the development and extension of microscopic physical theories. First, in the absence of a suitable theory, simulations provide a detailed microscopic picture of the properties of the system under study. This can be very useful in devising an appropriate theory. The phenomenological information gained in this way is often more useful, for the purposes of developing a theory, than experiments on real physical systems, due to the high level of detail and to the lack of uncertainty in the molecular structure and interactions. Secondly, when a microscopic theory does exist, the information from the simulations can be used to test the predictions of the theory, and possibly help to improve or extend it.

The interface simulations presented here can be used to illustrate both of these roles. At present, no microscopic theory is available that can predict the variation in the diffusion constant across an interfacial region. Hence, our present simulations on bcc systems, as well as those for the other systems, are important in providing a phenomenological base upon which such a theory could be built. In addition, the diffusion profiles, while not actually predicted, are necessary input functions to current microscopic theories of crystal growth from the melt.[17]

In contrast, a microscopic, first-principles theory, which claims to predict the structure and thermodynamics of crystal–liquid interfaces, was published some time ago. This theory is based on the density functional formalism and was developed by Haymet and Oxtoby.[27] The theory has since been improved and greatly extended in various ways by the work of McMullen and Oxtoby,[28] Curtin[30] and Moore and Raveché.[29] Despite the level of interest in this complex problem, the theory must still be considered to be in an embryonic stage of development, because the systems to which it may be applied are still limited. In particular, the theory cannot be tested against the present bcc simulations for a reason detailed below.

The crucial step in the development of a density functional theory (DFT) is to derive an expression for the free energy of an inhomogeneous molecular system as a functional of the single particle density $\rho(\mathbf{r})$. The equilibrium structure and thermodynamics of the system can then be determined by minimizing this free energy functional over

the space of physically realizable single particle density functions. Since an exact determination of this free energy functional is not possible at present, the functional is approximated by a Taylor expansion about a reference state whose properties are known. In this case, the reference state is the homogeneous liquid phase and the expansion coefficients are determined from the n-body direct correlation functions measured in this liquid phase. Because these correlation functions are not well known above $n = 2$, the expansion is generally truncated at this point.

Before the calculation of the interfacial properties can proceed, the density functional theory must be used to determine the equilibrium freezing properties of the system at the required temperature. The structure and thermodynamics of the coexisting liquid and solid phases are needed to determine the boundary conditions of the density profiles on either side of the interface. The equilibrium freezing calculation may be summarized as follows. First, the periodic single particle density of the solid is parametrized so that the minimization of the free energy functional can be performed. The most general parametrization for a given lattice type is the Fourier series

$$\rho(\mathbf{r}) = \rho_L \left[1 + \eta + \sum_{\{\mathbf{k}\}} \mu(\mathbf{k}) e^{i\mathbf{k}\cdot\mathbf{r}} \right], \tag{4}$$

where ρ_L is the bulk liquid density, η is the fractional density change on freezing, $\{\mathbf{k}\}$ represents the set of reciprocal lattice vectors (RLVs) corresponding to the particular lattice type under study, and $\rho_L\,\mu(\mathbf{k})$ is the Fourier component of the density corresponding to the wave vector $\mathbf{k}$. A simpler but less general parametrization that is commonly used expresses the density as a sum of Gaussian peaks centered at the lattice sites

$$\rho(\mathbf{r}) = \left(\frac{\alpha}{\pi}\right)^{3/2} \sum_i \exp(-\alpha|\mathbf{r} - \mathbf{R}_i|^2), \tag{5}$$

where the $\mathbf{R}_i$ are the real space lattice vectors, and α measures the width of the Gaussian peaks. For close packed systems, the Gaussian parametrization has been found to give almost identical freezing results as the more complicated but more general Fourier expansion.[33] After parametrization of the crystal density, the free energy (actually the grand potential difference between the solid and liquid) is minimized in such a way as to ensure the thermodynamic conditions of phase equilibrium are satisfied; that is, the pressure, temperature, and chemical potential of the crystal phase equal those of the liquid phase. The density $\rho(r)$ at the minimum is the equilibrium crystal density.

Once the equilibrium phases have been determined, a parametrization of the interfacial $\rho(\mathbf{r})$ is constructed by allowing the order parameters used in the equilibrium calculation to vary with z, the coordinate perpendicular to the interface. The shape of the z-dependent order parameter profiles, as well as the interfacial excess free energy, can then be determined from the minimization condition, together with the boundary conditions [the order parameters must tend toward the solid (liquid) equilibrium values as z goes to $+\infty(-\infty)$]. Many authors also assume that the Fourier components are slowly varying across the interface, which permits use of a square-gradient approximation.

The Fourier parametrization, used in the original paper by Haymet and Oxtoby,[27] is more general than the Gaussian, but is more complex. In practical calculations, the expansion for $\rho(\mathbf{r})$ must be truncated after the first few Fourier components. Hence Haymet and Oxtoby chose the bcc/melt interface to study because, unlike the fcc system (which at that time was the only crystal/melt system studied by simulation), it is possible to find physically reasonable solutions to the equilibrium freezing problem for a small numbers of Fourier order parameters. This very simple level of density functional theory predicts the 10–90 width of the fractional density change η for both the bcc (100) and (111) interfaces [the (110) was not studied] to be approximately given by

$$l_{10\text{-}90} \approx 3.7[-c''(k_1)]^{1/2}, \tag{6}$$

where $c''(k_1)$ is the second derivative of the *liquid* two-particle direct correlation function evaluated at the magnitude of the nearest neighbor RLV of the *solid*. For the inverse sixth-power potential bulk liquid at $\rho_l^* = 0.6833$ and $T^* = 0.1$, $c''(k_1)$ was measured in a simulation of 432 particles to be about $-1.17\sigma^3$. This leads to a 10–90 width of about 4.1σ or 6 and 10 lattice planes for the (100) and (111) interfaces, respectively. The splitting of the $\eta(z)$ and $\mu_1(z)$ profile, as described in Ref. 27, leads to a interfacial peak-height profile that would be slightly broader than this η profile, but by only at most a few tenths of σ. Hence this theory leads to interface widths which are similar to, but slightly smaller than, the widths measured in the present simulations.

Recent work on the density functional theory of solid–liquid interfaces has focused on the less complex Gaussian parametrization, which in principle provides a better representation of the bulk crystal freezing than a severely truncated Fourier expansion (but still less accurate than a full Fourier expansion). Moore and Raveché[29] make the ansatz that the single particle density of the interfacial system can be written

$$\rho(\mathbf{r}) = \rho_L + f(z)[\rho_s(\mathbf{r}) - \rho_L], \tag{7}$$

where ρ_L is the bulk liquid density, $\rho_s(\mathbf{r})$ is the bulk, spatially varying solid density [given by Eq. (5)], and $f(z)$ is a switching function that goes from 0 to 1 as the interface is traversed from the bulk liquid to the bulk solid. They then minimize a Helmholtz free energy functional (also using the square-gradient approximation) using a hyperbolic tangent parametrization of $f(z)$ to obtain the interfacial properties. Application of their theory to the fcc Lennard-Jones interface gives results that are very sensitive to the input parameters. The resulting range of results for a reasonable spread of input values does overlap with the simulations on this system, but is rather large, making comparison difficult.

McMullen and Oxtoby[28] have gone a significant step further by allowing the Gaussian width parameter α to vary with z. The form of this variation is determined by making the ansatz that the zero magnitude (bulk density) and first nonzero magnitude RLV Fourier components of $\rho(\mathbf{r})$ have shifted hyperbolic tangent profiles. This gives a four-parameter form (representing the widths and centers of the two profiles) for the single particle density. Minimizing the same grand potential functional used by Haymet and Oxtoby, without invoking the square-gradient approximation,

McMullen and Oxtoby examine the hard-sphere (111) interface. Although no hard-sphere crystal/melt interface simulations have been performed to make a direct comparison possible, the interfacial structure they obtain does compare very favorably with existing simulations of the Lennard-Jones interface. The same is true of the results of the interface theory by Curtin,[30] who minimized a grand potential functional (derived using a weighted density functional formalism) using a two parameter fit similar to that of McMullen and Oxtoby.

Unfortunately, none of these more recent density functional interface theories can be applied at present to the bcc inverse-power system. The reason for this is due not to flaws in the interface theories themselves, but rather to difficulties in the application to this bcc system of the underlying freezing theories on which the interface theories are based.[35,36] Hence, consistent boundary conditions for the interface calculation cannot be obtained, and direct comparison with the present simulations is not yet possible.

It has been shown recently that the density functional freezing theories which use a functional derived from a second-order perturbation expansion about a reference liquid phase (for example, the Haymet–Oxtoby theory[33] and a slight variation due to Baus and Colot[34]) do not predict a thermodynamically stable bcc phase for the $1/r^6$ system.[35,36] The bcc phases located by the functional are locally stable, but always less stable than the fcc phase. Moreover, the bcc phases exist only at unphysically high densities. It is possible that the addition of third-order terms to the functional expression could correct this situation. There is also the prospect that recent advances in choosing the reference system for the perturbation theory, developed by McCoy, Rick, and Haymet for quantum systems,[37] may lead to progress in this area. The DFT for freezing based on the weighted-density approximation (WDA) developed by Tarazona[38] and Curtin and Ashcroft,[39] on which the interface theory of Curtin[30] is based, has been used to predict the free energy of the hypothetical (and mechanically unstable) hard-sphere bcc solid,[40] but is not easily applicable to nonhard sphere systems in its present form. The original DF calculations, which used just several Fourier components for simplicity, certainly need to be extended. The present simulations are intended to provide both an incentive to explore further these theoretical issues, and "experimental" data with which to test candidate theories.

VI. CONCLUSIONS

We have performed molecular dynamics simulations of the bcc crystal/melt (100), (110), and (111) interfaces for a system of spherical particles interacting via an inverse-sixth-power potential. Using the 10–90 width of the density profile peak heights as a measure of the structural width, we find the three interfaces to be about 6, 9, and 7 molecular diameters wide, respectively. A measurement of the variation of the diffusion constant across the interface gives a 10–90 width for this quantity of about four molecular diameters for all of the interfaces studied. This is slightly wider than the diffusion width of 3σ seen in interfacial simulations of the Lennard-Jones system near its triple point.[13] That the bcc interface is broader is to be expected because the liquid to bcc transition is a "weaker" first-order phase transition than the liquid to fcc transition. [By the term "weaker transition" we mean one that has smaller discontinuities in the thermodynamic parameters (such as entropy and density) of the coexisting liquid and solid phases.]

Since this diffusion constant variation should be a more sensitive measure of the variation in molecular "environment" than the peak height width, we conclude that the width of the interfacial region (defined loosely as the region where particles can be said to be neither liquid-like or solid-like) is approximately the same for each of the interfaces studied. This lack of sensitivity of the diffusion width on the interfacial orientation has also been seen in the Lennard-Jones simulations.[13] The differences in both the peak-height widths and the overall shapes of the density profiles among the three interfaces are due primarily to the differences in the stacking geometries.

ACKNOWLEDGMENTS

This research was supported by the (U.S.) National Science Foundation and the Ford Motor Company through the PYI program.

[1] D. P. Woodruff, *The Solid–Liquid Interface* (Cambridge University, London, 1973).
[2] M. E. Glicksman and C. L. Vold, Acta Metall. **17**, 1 (1969).
[3] S. R. Coriell, S. C. Hardy, and R. F. Sekerka, J. Cryst. Growth **11**, 53 (1971); S. C. Hardy, Philos, Mag. **35**, 471 (1977).
[4] R. J. Schaefer, M. E. Glicksman, and J. D. Ayers, Philos, Mag. **32**, 725 (1975).
[5] B. Mutaftschiev and J. Zell, Surf. Sci. **12**, 317 (1968).
[6] G. Grange, R. Landers, and B. Mutaftschiev, J. Cryst. Growth **49**, 343 (1980).
[7] A. Bonissent and B. Mutaftschiev, Philos. Mag. **35**, 65 (1977).
[8] L. F. Rull and S. Toxvaerd, J. Chem. Phys. **78**, 3273 (1983).
[9] A. Bonissent and F. F. Abraham, J. Chem. Phys. **74**, 1306 (1981).
[10] A. J. C. Ladd and L. V. Woodcock, J. Phys. C **11**, 3565 (1978).
[11] J. N. Cape and L. V. Woodcock, J. Chem. Phys. **73**, 2420 (1980).
[12] J. Q. Broughton, A. Bonissent, and F. F. Abraham, J. Chem. Phys. **74**, 4029 (1981).
[13] J. Q. Broughton and G. H. Gilmer, J. Chem. Phys. **84**, 5749 (1986).
[14] G. Bushnell-Wye, J. L. Finney, and A. Bonissent, Philos. Mag. A **44**, 1053 (1981).
[15] O. A. Karim and A. D. J. Haymet, J. Chem. Phys. **89**, 6889 (1988).
[16] F. F. Abraham and J. Q. Broughton, Phys. Rev. Lett. **56**, 734 (1986).
[17] T. Munakata, J. Phys. Soc. Jpn. **43**, 1723 (1977); see also **45**, 749 (1978).
[18] W. G. Hoover, *Molecular Dynamics* (Springer, New York, 1986).
[19] B. J. Alder and T. E. Wainwright, J. Chem. Phys. **27**, 1208 (1957).
[20] A. Rahman, Phys. Rev. A **136**, 405 (1964).
[21] L. Verlet, Phys. Rev. **159**, 98 (1967).
[22] M. Karplus, Phys. Today **40** (5), 68 (1987).
[23] W. W. Wood, in *Fundamental Problems in Statistical Mechanics*, edited by E. D. G. Cohen (North-Holland, Amsterdam, 1975), Vol. 3, p. 331.
[24] W. C. Swope, H. C. Anderson, P. H. Berens, and K. R. Wilson, J. Chem. Phys. **76**, 637 (1982).
[25] J. Hansen and I. McDonald, *The Theory of Simple Liquids* (Academic, New York, 1976).
[26] W. G. Hoover, M. Ross, K. W. Johnson, D. Henderson, J. A. Barker, and B.C. Brown, J. Chem. Phys. **52**, 4931 (1970).
[27] A. D. J. Haymet and D. W Oxtoby, J. Chem. Phys. **74**, 2559 (1981); D. W. Oxtoby and A. D. J. Haymet, *ibid.* **76**, 6262 (1982).

[28]W. McMullen and D. W. Oxtoby, J. Chem. Phys. **88**, 1967 (1988).
[29]S. M. Moore and H. R. Raveché, J. Chem. Phys. **85**, 6039 (1986).
[30]W. Curtin, Phys. Rev. Lett. **59**, 1228 (1987).
[31]B. B. Laird and A. D. J. Haymet, Materials Research Society Symposia Proceedings **63**, 67 (1986).
[32]B. J. Alder and T. E. Wainwright, Phys. Rev. A **1**, 18 (1970); J. Phys. Soc. Jpn. Suppl. **26**, 267 (1968).
[33]B. B. Laird, J. D. McCoy, and A. D. J. Haymet, J. Chem. Phys. **87**, 5449 (1987).
[34]M. Baus and J. L. Colot, Mol. Phys. **55**, 653 (1985).
[35]Steven W. Rick (private communication).
[36]J. L. Barrat, J. P. Hansen, G. Pastore, and E. M. Waisman, J. Chem. Phys. **86**, 6360 (1987).
[37]J. D. McCoy, S. W. Rick, and A. D. J. Haymet, J. Chem. Phys. **90**, 4622 (1989).
[38]P. Tarazona, Mol. Phys. **52**, 81 (1984).
[39]W. A. Curtin and N. W. Ashcroft, Phys. Rev. A **32**, 2909 (1985).
[40]W. A. Curtin and K. Runge, Phys. Rev. A **35**, 4755 (1987).